Electronics and Electrical Engineering

http://www.aimspress.com/journal/ElectronEng

AIMS Electronics and Electrical Engineering, 2(1): 27–36
DOI: 10.3934/ElectrEng.2018.1.27
Received: 16 May 2018
Accepted: 09 July 2018
Published: 13 July 2018

Research article

Thermal conductivity survey of different manufactured insulation systems of rectangular copper wires

Martin Seilmayer* **and Varun Kumar Katepally**

Department of Magnetohydrodynamics, Institute of Fluid Dynamics, Helmholtz-Zentrum Dresden-Rossendorf, Dresden, Germany

* **Correspondence:** Email: m.seilmayer@hzdr.de.

Abstract: Especially in high power applications, thermal design of magnetic field coils is a critical part of efficient electromagnetic system design. Since thermal expansion of the coil effects magnetic field geometry, temperature drop across the windings should be kept as low as possible. Here the insulation system between wires guides ohmic heat to the surface of the coil and influences the total thermal performance. Because of very less information about the general thermal performance and quality of manufactured multilayer insulation systems, the present survey investigates several variants made of enameled wires and Polyimide film wrapped wires. Hereby, different joining technologies like bonding or backfilling determine the thermal conductivity, which obviously differs from values of individual raw materials. Best performance could be gained with a Kapton®–CR film wrapped wire, backfilled with high thermal conductivity resin. Finally, the survey concludes that manufactured insulation systems drop approximately ten to twenty percent of the thermal conductivity, which could be theoretically achieved by an optimal layer composition of individual raw materials.

Keywords: power cable thermal factors; insulation thermal factors; thermal insulation

1. Introduction

A large scale Taylor-Couette (TC) experiment with liquid sodium as working fluid, investigates shear flow instabilities in presence of magnetic fields. Herein, classic TC setup consists of a cylindrical gap filled with the liquid of interest between two concentric and differentially rotating cylinders. The experiment is mainly motivated by a geo- and astrophysical effect called magneto-rotational instability (MRI) [1, 2, 3, 4]. Since its standard version depends only on an axial magnetic field B_z and differential rotation $\partial\Omega/\partial r$, a meter scale size ($h = 2\,\mathrm{m}$, $r_\mathrm{i} = 0.2\,\mathrm{m}$, $r_\mathrm{o} = 0.4\,\mathrm{m}$) is required to bring down the parameter range to achievable laboratory conditions.

In such a large cylinder geometry, sufficiently excited standard MRI requires an axial magnetic

field in the order of $B_z = O(100\,\mathrm{mT})$. This can be generated by an optimized cylindrical coil which is $H = 3\,\mathrm{m}$ in height and $D \approx 1.5\,\mathrm{m}$ in diameter. The design goal is a homogeneous distributed field in the cylindrical gap volume with $B_{z,\max} = 150\,\mathrm{mT}$. In consequence of the large coil volume, a total power of the magnetic field system of about $P \approx 120\,\mathrm{kW}$ (with $U = 400\,\mathrm{V}$ and $I = 300\,\mathrm{A}$) is required. In order to keep the thermal expansion and corresponding geometric changes due to ohmic warming at a minimum, the question of proper heat transport in the constructive design needs to be answered.

In general, a cylindrical coil system is built of wound wires where each wire surface made of an insulation material is in touch with neighboring wire surfaces. As electrical current flows through the wire, the insulation system realizes electrical insulation and mechanical self-support. Besides that, it guides dissipated ohmic heat through the insulation radially outward into a cooling system or to environment.

The thermal design of a magnetic field coil in the assumed power range strongly depends on the thermal performance of the insulation system. The latter is defined by the insulation material, geometry of insulation (dense packed with square wires or patchy packed with round wires) and the manufacturing process itself, which sets the quality of interconnection between two insulation layers. Here thermal and mechanical stress, like duration of thermal bonding, pressure or activation of surface will influence the overall thermal performance. Additional effects like delamination or assembly clearances, effects of polymerization, entrapped particles and other parasitics lower the thermal performance as well. For example $\lambda_{\mathrm{PAI}} \approx 0.26\,\mathrm{W/(m \cdot K)}$, which is a typical value for Polyaminde / -Imide as raw material, is hardly representing the thermal conductivity value for the entire insulation system because of the effects mentioned above. Besides that, the chosen insulation system also limits the electrical, mechanical and temperature conditions of operation.

Because of the amount of electrical power needed the proposed coil design requires large cross sectional rectangular wires with $A > 9.6\,\mathrm{mm}^2$ area. Finally, there are two possible flavors, enameled wires and film wrapped wires which have to be considered.

Enameled wires If we talk about reasonable geometric precision of final multilayer coil geometry, the variance of insulation thickness for wires with rectangular cross section in grade 1 is rather large ($d_{\mathrm{iso}} = 60 \ldots 100\,\mu\mathrm{m}$), with respect to DIN EN 60317-2 [6]. However, the fundamental manufacturing process of coils made from wires can be split in two steps: first winding the coil geometry and second strengthening the winding package. In case of enameled wires, the second manufacturing step finalizes insulation system by; i) baking / bonding or ii) (vacuum) filling and hardening. In both variants the processed insulation system gains mechanical stiffness and thermal conductivity. With respect to chemical properties, thermal bonding (typically $\vartheta \approx O(200^\circ\mathrm{C})$ for some hours) introduces thermal stress which starts polymerization on the interfacing wire surfaces, which coalesce and bond the individual wire insulation in the end. For example Polyimide PS / QT [13] is such a common insulation material which can be processed in the described way.

Next to that, we find some variants of Polyesterimide enameled wires, which cannot be bond by thermal impact. Here a vacuum filling with a resin (e. g. NP1025 [12]) is advised to close the residual gaps in between the winding package. Here the insulation system is additionally determined by layer thickness and thermal characteristics of the filler or glue.

However, insulation systems made of enamelled wires consist of only a few material layers which easily sustain changing mechanical or electrical loads.

Table 1. Selection of insulation materials.

Name	Species	$\frac{\lambda}{\mathrm{W/(m\cdot K)}}$	$\frac{T_\mathrm{D}}{^\circ\mathrm{C}}$	$\frac{k}{10^6}$	$d_\mathrm{iso}/\mu\mathrm{m}$	Remarks
PU	Polyurethan	0.25 . . . 0.5	95	100	60 . . . 100	[5]; private com. Mr. B. Krause (Elektrisola GmbH)
PAI–Lack	Polyamid/imide	0.26 . . . 0.54	200 . . . 260	25	60 . . . 100	[6, 7]
Kapton MT+	Polyimide - Film	0.78	> 200	17	100	[8, 9]
Kapton 150PRN411	10 µm FEP – 25 µm Kapton – 2.5 µm FEP	≈ 0.12	> 200	17	150	TB [9]
200FN919	12.7 µm FEP – 25.4 µm Kapton – 12.7 µm FEP	≈ 0.12	> 200	17	200	TB [9]
100FCRN019		≈ 0.38	> 200	17	150	[9, 10]
Teflon	FEP	0.19 . . . 0.24	150 . . . 200	83 . . . 104	12.5	[7]
Thermal bond	Polyamid	≈ 0.24	80 . . . 160	95	100	
	PVB	≈ 0.22		155	100	[11]
Resin filler	NP1025	≈ 1.3	< 180°C	30	10	possible filler, [12]

*Note: TB–Thermal bonding; λ–thermal conductivity; T_D–maximum usage temperature; k–expansion coefficient at $T < 100^\circ$C, compare with copper $k_\mathrm{Cu} = 17.3 \cdot 10^{-6} \cdot \mathrm{K}^{-1}$; d_iso–insulation thickness, typical values.

Polyimide film wrapped wires The most famous Polyimide film brand is DuPond™Kapton®. This special tape has outstanding electrical insulation capabilities and some types of Kapton® provide excellent thermal conductivity as well, like Kapton®–MT+ [8] or Kapton®–CR [10]. Kapton® film is available with a minimum thickness of $d = 25\,\mu$m. Because of its rather bad wetting properties, the film surface has to be activated and coated with FEP (Teflon) to achieve proper contact with a copper surface. A multi layer system (e. g. FEP–Kapton®–FEP, like 200FN919) is first (thermally) laminated on copper wire surface with an overlap of less than 50% in one or two layers. Because of the geometric structure caused by the overlap, delamination cannot be prevented entirely in a first instance.

Provided a sufficient mechanical preload on the wire, the delaminated areas can be closed by thermal bonding or filling in the subsequent winding process step. In contrast to the bonding, where FEP layer melts and squeezes into the open gaps, the vacuum filling process with resin may also prevent the coil from thermal impact during manufacturing, because the hardening takes place at room temperature.

The present work discusses thermal conductivity of different available industrial materials processed into insulation systems. For a better comparison with achieved results, Table 1 gives an overview of different common insulation (raw) materials.

2. Experimental setup

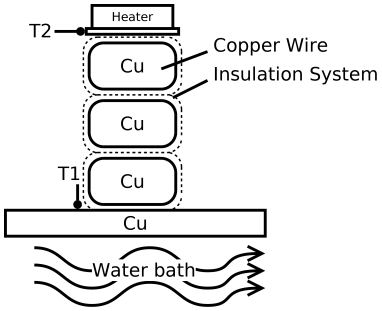

(a) Measurement principle

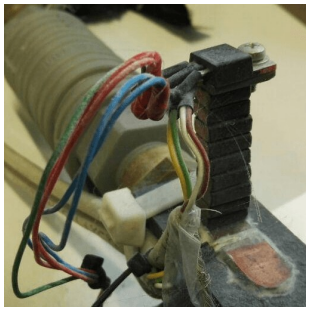

(b) Magnebond AB–220

(c) Magnetemp CA–200

(d) Thermal bonding connects only at the periphery of the wire.

Figure 1. Experimental setup. The principle of direct measurement is given in (a). Sub figures (b) and (c) display two realizations. The outer insulation wool is filled with Aerogel providing best thermal insulation. Figure (d) gives an illustration of the quality of thermal bonding. It becomes clear, that the wire insulation only merges at its periphery.

To determine the thermal conduction λ of processed insulation systems, a direct measurement approach according to Figure 1a was applied. In the present case a transistor is used as heater element, which enables high accuracy and easy mounting. The whole heater system is a house development and can deliver up to $P = 100\,\mathrm{mW} \pm 0.5\%$ of heat power [14]. The applied heat sinks in a water bath with constant temperature, which can be assumed as thermal "ground". The heat sink itself is a copper inlet embedded in a hollow PVC bar which is flushed with a stream of water with constant temperature. The water is supplied by a controlled thermostat from Lauda with a control loop precision of $\delta T \approx 0.01\,\mathrm{K}$. The differential temperatures are taken by PT100 sensors, which are positioned in the copper heat sink (water bath) and right below the transistor. The value of temperature drop $\Delta\vartheta$ is taken approximately 10 min after the initial power application. This ensures a steady state condition and a homogeneous heat distribution in the sample.

The thermal conductivity of an insulation system depends on the chosen material (see Table 1), layer setup and the manufacturing process. To cover varying combinations, different wire samples from industrial production were processed into a stack of wire pieces with several insulation layers in between. Table 3 summarizes all available samples which cover the variants discussed above.

In the following sections the investigated insulation materials will be introduced.

Magnebond AB-220 [15] This is a PAI-enamel based on Polyamide-Imide with a temperature classification of 220°C. The outer layer consists of an aromatic Polyamide thermal bond enamel. The wrapped wires of a coil are packed together with a baking like process in an oven. This creates a frictional self-supporting coil. Impregnation during the manufacturing process is not necessary.

Magnetemp CA-200 [16] This is a THEIC* modified Poliesterimide, which is additionally over coated with polyamide-imides. The system is optimized for fast automated production processes and provides self-lubricating properties. There is also a variation Magnetemp CA_2-200, which is silicone-free and has reduced lubricating properties.

Kapton® film In a wrapping process, a polyimide film is wrapped around the pure copper wire with an overlap of $< 50\%$ (customer specified). Due to the overlap, a filling material (resin, glue) is always added during the processing. Once hardened, the filler achieves mechanical and thermal connection between the coil layers. In the simplest case this is some sort of adhesive. To simulate a common material sample no. 8 was prepared with VA20 [17] which provides a thermal conductivity of $\lambda_{\mathrm{VA20}} \approx 0.1\,\mathrm{W/(m \cdot K)}$. The target system of the final coil design will be manufactured with a special backfiller resin (NP1025 [12] with $\lambda_{\mathrm{NP1025}} \approx 1.3\,\mathrm{W/(m \cdot K)}$).

Table 2. Flavors of manufacturing

Wire type			Bonding type
Abbr.	enameled	wrapped film	
B1	•	–	thermal 4 h at 250 °C
B2	•	–	thermal 4 h at 300 °C
G	•		VA20 [17], glued
K1	–	•	NP1025, backfilled
K2	–	•	VA20, glued

Creation of the insulation system Prior to the measurements, the insulation system has to be set-up. To achieve this, 1 cm long wire pieces are prepared by different methods, which are finally stacked and pressed. There are two major ways to create the insulation system. First, samples might be "baked" in an oven, which describes best the thermal bonding procedure. This type of sample is abbreviated with "B1" or "B2", depending of the exact conditions. The non-thermal types of preparation are coded with "G" and "K" according to Table 2 which summarizes the different kinds of preparation procedures applied.

*the use of tris-2-hydroxyethyl iso-cyanurate increases the softening temperature

Table 3. Sample parameters

Nr	Name	b/mm	h/mm	d_{Iso}/mm	N	Type
1	Magnebond AB-220	6.7	3.75	0.17	9	PAI
2	Magnetemp CA 200	8.0	5.60	0.11	4	THEICmod PAI
3	Magnetemp CA 200	8.0	5.60	0.11	4	THEICmod PAI
4	Magnetemp CA 200	8.0	5.60	0.11	3	THEICmod PAI
5	Kapton CR + NP1025	9.2	2.65	0.22	10	Kapton
6	Magnetemp CA 200	16.0	5.60	0.11	5	THEICmod PAI
7	Magnetemp CA 200	16.0	5.60	0.11	4	THEICmod PAI
8	Kapton + VA20	4.8	2.00	0.26	5	Kapton
9	Magnebond AB-220	5.6	3.55	0.15	5	PAI
10	Magnebond AB-220	8.0	3.85	0.16	5	PAI

*Note: All copper wires with dimensions $b \times h$ were cut in 1 cm long pieces. The insulation thickness d_{iso} has been measured individually and differs from standard. In all measurements thermal heat power of $P = 100\,\mathrm{mW}$ was injected.

As a major result of this preparation, Figure 1d depicts an example for the systematic defective connection for methods "B1" and "B2". Here the wire insulation only bond at the outer regions of the geometry caused by a "bone"-like cross section preventing an equal bond. The reason for that is the edge recession effect, which originates from the coating process when manufacturing the wire. Even if the cross-section has comfortable rounded corners, surface tension gradients attract the liquid enamel here, which lead to a thinning of the coating layer directly at the corner whereas a thickening a side can be observed [18]. This typical edge recession effect is noticeable as a bulging thickening like the "bone"-like cross section mentioned above. As a consequence of that, an assembly clearance appears, so that a delaminated area between the two surfaces is created – as seen in Figure 1d. Subsequently, the thermal performance would be influenced by entrapped thin layers of gas. Due to the usage of liquid fillers like glue (VA20) or resin (NP1025) such assembly clearance can be backfilled to improve thermal conductivity.

A minor question addresses thermal stability of the enamel itself. Would it change its thermal conductivity after a strange heat-up or not. Although Magnetemp CA-220 is not suited for thermal bonding, three different samples (no. 2, 3, 6) were made to get some clarification.

Insulation thickness is measured for each wire separately, it turns out that values differ significantly in comparison to given numbers by the manufacturer or standard DIN EN 60317-2 [6].

3. Determining thermal conductivity

The thermal conductivity can be determined by the law of one dimensional heat conduction

$$\dot{Q} = \frac{A \cdot \Delta\vartheta}{\sum_i \frac{d}{\lambda_i}}, \tag{3.1}$$

where the heat flow $\dot{Q}$ have to pass a number N of different layers of material with cross sectional area A. The thermal conductivity of the insulation layer is then given by

$$\lambda_{\mathrm{Iso}} = \frac{N \cdot d_{\mathrm{Iso}}}{b \cdot l \cdot \frac{\Delta\vartheta}{\dot{Q}} - N\frac{h}{\lambda_{\mathrm{Cu}}}}, \tag{3.2}$$

where b and h determine the dimensions of the wire sample with the length l. The parameter d_{Iso} was measured in advance. The material property of copper is given by $\lambda_{\mathrm{Cu}} = 393\,\frac{\mathrm{W}}{\mathrm{m\cdot K}}$ [19]. Finally, the heat loss of the transistor equals to the conducted heat in the wire stack, so $P = \dot{Q}$ can be assumed. In general, the term $N\frac{h}{\lambda_{\mathrm{Cu}}}$ in equation (3.2) summarizes *all* layers of the system expect the insulation system, e. g. heat transfer paste to connect the transistor on top. A brief comparison of the two terms in the denominator for sample no. 2 with $b \times h \times l = 8 \times 5.6 \times 10\,\mathrm{mm}^3$

$$\begin{aligned} b \cdot l \cdot \frac{\Delta\vartheta}{\dot{Q}} &\overset{?}{\gg} N\frac{h}{\lambda_{\mathrm{Cu}}} \\ (8 \cdot 10)\ \mathrm{mm}^2 \cdot \frac{4\,\mathrm{K}}{0.1\,\mathrm{W}} &\gg 4 \cdot \frac{5.6\,\mathrm{mm}}{393\,\mathrm{W/(m \cdot K)}} \\ 3200\,\mathrm{mm}^2 \cdot \frac{\mathrm{K}}{\mathrm{W}} &\gg 57\,\mathrm{mm}^2 \cdot \frac{\mathrm{K}}{\mathrm{W}}, \end{aligned} \tag{3.3}$$

shows, that λ_{Iso} is mainly influenced by the temperature drop $\Delta\vartheta = T_2 - T_1$ than the rest (here copper). Even if we encounter heat transfer paste with typical values $d_{\mathrm{HTP}} \approx 0.1\,\mathrm{mm}$ and $\lambda_{\mathrm{HTP}} = 5\,\mathrm{W/(m \cdot K)}$ on both sides of the stack, the corresponding value would be in the order of $2 \cdot \frac{h}{\lambda_{\mathrm{HTP}}} \approx 100\,\mathrm{mm}^2 \cdot \mathrm{K/W}$, which is still much less compared to the left side. Thermal losses to the environment are not considered, because of excellent Aerogel insulation.

4. Results

As a general result the delamination tendency of enameled wires must be mentioned. Even a high pressure during baking, could not prevent this effect which definitely influences thermal performance of the insulation system. Next to that, the insulation thickness was always different from the standard or values given in personal communication. The individual probing of that parameter was indispensable.

The main result of the present survey is given in Table 4. In comparison with Table 1, Magnetemp CA-200 performs worst. It did not reach the theoretical value from PAI-enamel or related materials. A not acceptable thermal bond procedure might improve the thermal conductivity, but destroys the insulation in the same moment (sample no. 3). Here electrical shortcuts could be detected. In contrast to that, the thermal bonding procedure with Magebond AB-220 always leads to much better performance.

The wrapped film insulation systems strongly depend on the filler and layer size. Sample no. 8 consists of an unknown Polyimide film insulation (we guess Kapton®–CR). The sample consists of 6 layers and its calculated thickness is the measured mean. With the assumption of Kapton®–CR and VA20 as filler, the theoretical value of thermal conductivity can be estimated by

$$\lambda_{\mathrm{K-un}} = \frac{d_{\mathrm{iso}}}{\frac{d_{\mathrm{Kapton}}}{\lambda_{\mathrm{CR}}} + \frac{d_{\mathrm{VA20}}}{\lambda_{\mathrm{VA20}}}} \tag{4.1}$$

$$= \frac{0.26\,\text{mm}}{\frac{200\,\mu\text{m}}{0.385\,\text{W/(m·K)}} + \frac{60\,\mu\text{m}}{0.1\,\text{W/(m·K)}}}$$
$$\approx 0.23\,\text{W/(m}\cdot\text{K)}.$$

Here, the reached value in the measurement was $\lambda_{\text{K-un}} \approx 0.19\,\text{W/(m}\cdot\text{K)}$, which remains below the theoretical value.

The best result was gained by sample no. 5, a Kapton®–CR system backfilled with NP1025 resin. The sample was manufactured within an industrial process. It reached a thermal conductance of the insulation system of $\lambda_{\text{KNP}} \approx 0.42\,\text{W/(m}\cdot\text{K)}$. For comparison, the theoretical value might be calculated from geometry parameters in the same way shown above. The assumed value of

$$\lambda_{\text{KNP-th}} = \frac{d_{\text{iso}}}{\frac{d_{\text{Kapton}}}{\lambda_{\text{CR}}} + \frac{d_{\text{NP1026}}}{\lambda_{\text{NP1025}}}} \tag{4.2}$$
$$= \frac{0.22\,\text{mm}}{\frac{160\,\mu\text{m}}{0.385\,\text{W/(m·K)}} + \frac{60\,\mu\text{m}}{1.3\,\text{W/(m·K)}}}$$
$$\approx 0.48\,\text{W/(m}\cdot\text{K)}$$

is also higher than the result of measurement.

Table 4. Measured thermal conductance.

Name	No.	$\Delta\vartheta$/K	$\frac{\lambda}{\text{W/(m·K)}}$	Process
Magnetemp CA 200	4	3.46	0.121	G
Magnetemp CA 200	7	2.44	0.114	G
Magnetemp CA 200	3	2.85	0.198	B2
Magnetemp CA 200	2	4.01	0.140	B1
Magnetemp CA 200	6	2.93	0.119	B1
Magnebond AB-220	1	8.34	0.278	B1
Magnebond AB-220	9	4.09	0.221	B1
Magnebond AB-220	10	3.02	0.224	B1
Kapton CR + NP1025	5	3.85	0.419	K1
Kapton + VA20	8	9.48	0.191	K2

Like all measurements the determined values are subject to uncertainties. The random errors of all length measurements are estimated with $\Delta d = \pm 5\,\mu\text{m}$, which is a typical value for micrometer gauges. Temperatures can be measured with a precision of $\Delta\Delta\vartheta = \pm 0.1\,\text{K}$ and the heat source gained 0.5% accuracy. The exactness of λ_{Cu} is not known from the datasheet, but we assume $\Delta\lambda_{\text{Cu}} = \pm 1\,\text{W/(m}\cdot\text{K)}$. Taking the geometric sum of all partial differentials

$$\sqrt{\sum_i \left(\frac{\partial\lambda(x_i)}{\partial x_i}\cdot\Delta x_i\right)^2} = \Delta\lambda_{\text{iso}}, \tag{4.3}$$

lead finally to a relative error of less than $\Delta\lambda_{\text{iso}}/\lambda_{\text{iso}} < 6.3\%$. However, $\partial\lambda_{\text{iso}}/\partial d_{\text{iso}}$ affects the result most, so d_{iso} has to be determined as precise as possible. Next to that, two important systematic main

effects will be mentioned in the following. First, the insulation layer structure cannot be resolved exactly in terms of delamination, imbedded materials or other homogeneity. In consequence the theoretical values from equations (4.1) and (4.2) remain estimates for ideal conditions. Second, the presented measurement technique is a direct measurement of λ, so uncertainties in temperature measurement or the loss of heat because of broken insulation might additively affect the final result. One candidate of this category are the connection wires of the transistor as well as the measurement cables of the PT100 sensors, which sink some heat power. To minimize this effect the temperature of the heater and its temperature sensor was set approximately to room temperature. Subsequently, water baths temperature was fixed accordingly some degrees below.

5. Conclusions

High power magnetic field systems, like the introduced 120 kW– finite cylinder coil do need a proper thermal design to achieve lowest geometric heat expansion and exact thermal boundary conditions. Due to lack of information about the thermal conductivity of manufactured insulation systems, the present survey was motivated. Different industrial insulation materials were investigated, e. g. Magnetemp CA-200, Magnebond AB-220 and different types of Kapton®–film wrapped wires. Since, enameled wires in a thermal bond process tend to delaminate which distorts thermal design, the application of fillers is recommended, especially in a vacuum manufacturing process to release all gas out of the winding package.

Next to that, samples of Kapton®–film wrapped wires outperform enameled wires if high thermal conductive films (e. g. Kapton®–CR or Kapton®–MT+) and appropriate fillers are used. The best result with approximately $0.42\,\mathrm{W/(m \cdot K)}$ was determined with such a layer composition.

In comparison with unprocessed (raw) material values, the achieved thermal conductivity in a processed insulation system seems to be about 10% . . . 20% less than the theoretical best possible value. This drop of thermal conductivity should be considered in a coil design.

Acknowledgements

The present paper is a result of the vertical field coil design of DRESDYN MRI/TI project which is supported by Helmholtz-Zentrum Dresden-Rossendorf. The authors like to thank Partsch GmbH for the great support in coil and insulation design. Special thanks goes to Essex Inc. for supplement of industrial samples.

Conflict of interest

The Authors state that there is no conflict of interests.

References

1. Rüdiger G and Schultz M (2006) The Magnetorotational Instability of MHD Taylor-Couette Flows. *Magnetohydrodynamics* 42: 3–11.
2. Michael DH (1954) The stability of an incompressible electrically conducting fluid rotating about an axis when current flows parallel to the axis. *Mathematika* 1: 45–50.

3. Velikhov EP (1959) Stability of an ideally conducting liquid flowing between rotating cylinders in a magnetic field. *Soviet physics / JETP* 36: 995–998.
4. Balbus SA and Hawley JF (1991) A powerful local shear instability in weakly magnetized disks. I-Linear analysis. II-Nonlinear evolution. *The Astrophysical Journal* 376: 214–233.
5. Druflon Electronics P Ltd (2017) Properties of PTFE and Some Other Insulating Materials, Ghaziabad, India. Available from: `http://www.druflon.com/ptfeprop.html`.
6. DIN EN 60317 – Specifications for particular types of winding wires (2011) Deutsche Norm DIN EN 60317.
7. Professional Plastics Inc and Kietzke C (2008) Thermal Properties of Plastic Materials, Datasheet, Fullertron, USA.
8. DuPond (2016) DUPONT™ KAPTON® MT+ – Thermally Conductive Polyimide Film, Datasheet, DuPont, Wilmington, Delaware, USA.
9. DuPond (2017) DUPONT ™ KAPTON® – Summary of Properties, Datasheet, DuPont, Wilmington, Delaware, USA.
10. DuPond (2000) Corona Resistant Kapton CR Takes Electrical Insulation Design and Reliability to New Levels, Datasheet, DuPont, Wilmington, Delaware, USA.
11. Eastman Chemical Company (2014) Saflex® DG PVB Zwischenschicht für den konstruktiven Glasbau, Datasheet, Saflex.
12. ALH Systems Limited (2015) NP1025 – HIGH THERMAL CONDUCTIVITY EPOXY RESIN SYSTEM, Datasheet, Westbury, England.
13. Schildbach G (2017) Lacke im Vergleich. Available from: `https://www.elektrisola.com/de/backlackdraht/backlack-typen/lacke-im-vergleich.html`.
14. Seilmayer M and Katepally VK (2017) On an Analog Controlled Precision Heat Power Source, *IOP Conference Series: Materials Science and Engineering* 228: 012024.
15. Essex Inc (2010) MAGNEBOND AB-220, Datasheet.
16. Essex Inc (2010) MAGNETEMP CA-200, Datasheet.
17. WEICON GmbH & Co KG (2017) Contact VA20, Datasheet, Münster. Available from: `www.weicon.de`.
18. Römpp H and Adler HJP (1998) *Römpp-Lexikon Lacke und Druckfarben*, Stuttgart: Thieme.
19. Deutsches Kupfer Institut (2015) Cu-OFE – DKI Werkstoff-Datenblätter, Datasheet, Deutsches Kupfer Institut, Düsseldorf.

AIMS Press